Efficient Identification of Different Types of Carbons in Organic Solids by 2D Solid-State NMR Spectroscopy

ARTICLE *in* THE JOURNAL OF PHYSICAL CHEMISTRY A · SEPTEMBER 2011

Impact Factor: 2.69 · DOI: 10.1021/jp2071293 · Source: PubMed

7 AUTHORS, INCLUDING:

Rongchun Zhang
University of Michigan
27 PUBLICATIONS **122** CITATIONS

SEE PROFILE

Pingchuan Sun
Nankai University
119 PUBLICATIONS **1,539** CITATIONS

SEE PROFILE

THE JOURNAL OF PHYSICAL CHEMISTRY A

ARTICLE

pubs.acs.org/JPCA

Efficient Identification of Different Types of Carbons in Organic Solids by 2D Solid-State NMR Spectroscopy

Rongchun Zhang,[‡] Xin He,[†] Weigui Fu,[‡] Tiehong Chen,[†] Pingchuan Sun,*[,†] Baohui Li,*[,‡] and Datong Ding[‡]

[†]Key Laboratory of Functional Polymer Materials, Ministry of Education, College of Chemistry and [‡]School of Physics, Nankai University, Tianjin 300071, People's Republic of China

Supporting Information

ABSTRACT: An efficient method for identifying different types of carbon groups (CH_3, CH_2, CH, and quaternary carbons) in organic solids is proposed by utilizing the combination of a two-dimensional (2D) $^{13}C-^{1}H$ polarization inversion spin exchange at magic angle (PISEMA) NMR experiment and numerical simulation results of simple isolated $^{13}C-^{1}H$ dipolar coupling models. Our results reveal that there is a unique line shape of the $^{13}C-^{1}H$ dipolar splitting pattern and a corresponding characteristic splitting value for each carbon group, based on which different carbon types can be distinguished unambiguously. In particular, by using this method, the discrimination and assignment of overlapped signals from different types of carbons can be achieved easily. The efficacy of this method is demonstrated on typical solid small molecules, polymers, and biomacromolecules.

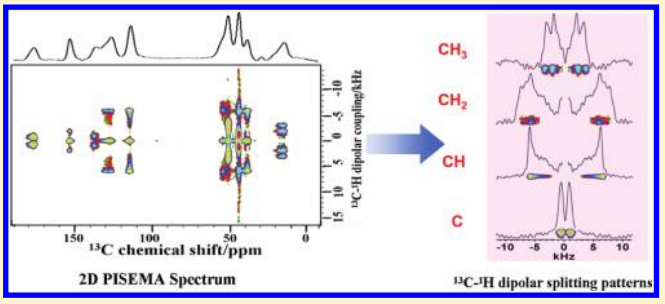

1. INTRODUCTION

The emergence of cross polarization (CP), magic angle spinning (MAS), and other efficient methods of proton decoupling has made it routine and easy for the acquisition of ^{13}C solid-state NMR spectra with high resolution and sensitivity.[1−3] These methods can be quite efficiently used to obtain the microstructure and dynamics information of organic solids in cases where each peak of the spectra can be clearly identified and assigned.[4−8] In solution NMR, CH_n (n = 3, 2, 1, and 0, corresponding to CH_3, CH_2, CH, and quaternary carbons, respectively) signals are generally resolved based on J-couplings by the attached-proton test (APT)[9] or distortionless enhancement by polarization transfer (DEPT)[10] due to the narrow line width of each peak. However, in solid-state NMR, the line width of peaks is greatly broadened by widespread dipolar interactions and chemical shift anisotropy. Furthermore, as no universal rules are suitable for treating all of them, the extraction and identification of CH_n signals is much more difficult. Hence, the identification of CH_n groups has long been a challenge, especially in polymers and biomacromolecules. Despite these challenges, great progress has been made in recent decades. A novel method based on the J-coupling technique in solution NMR was first extended to the crystalline systems with a long transverse relaxation time and resolved spectral lines.[11,12] A combination of polarization, polarization inversion, and spin depolarization techniques was also reported to achieve clean selection of quaternary carbons and CH_2 signals in noncrystalline solids, and then, the CH and CH_3 signals were edited by a linear combination of several spectra with partial selectivity.[13−16] However, the experiments have to be done at low or moderate MAS rates to make sure that the spin dynamics of four groups will not be affected, which also reduce the spectral resolution to a great extent. Using the ideal short-term heteronuclear local field evolutional behaviors of ^{13}C spins in the absence of multiple-pulse homonuclear decoupling, the differentiation among C/CH_3, CH, and CH_2 groups can also be achieved.[17] Almost at the same time, the dipolar-based recoupled polarization transfer (REPT) method was proposed to identify CH and CH_2 signals relative to that of quaternary carbons and CH_3.[18] Shortly afterward, the special dipolar-dephasing properties of multiple-quantum coherence was utilized to yield pure CH and CH_2 spectra.[19,20] Although the above novel techniques have many advantages, all of the techniques suffered from a relatively low signal-to-noise ratio compared to the full CP/MAS signal, typically around 10%.[20]

Since the concept of separated local field (SLF) was put forward,[21−23] SLF techniques have been widely studied both in theory and experiments over the past few decades.[24−27] As one of the most powerful SLF techniques, the two-dimensional (2D) polarization inversion spin exchange at magic angle (PISEMA) technique[24] enjoys greatest popularity in probing the structure and dynamics of materials. It has been commonly used to determine the order parameters of liquid crystals[28,29] or provide the amplitude and geometry of molecular motions in organic solids.[30,31] The pulse sequence of PISEMA shown in Figure 1 provides the best resolution of the heteronuclear dipolar splitting for powder solids among the SLF techniques.[28,32] Notably, the

Received: July 26, 2011
Revised: September 7, 2011
Published: September 08, 2011

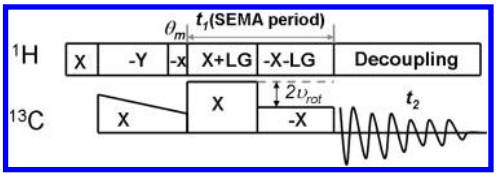

Figure 1. Pulse sequence for the 2D PISEMA experiment,[28] in which the LG homonuclear decoupling pulse sequence is used in the SEMA period and the phase-alternated ^{13}C RF field strengths are carefully adjusted so that the difference in amplitude is equal to $2\nu_{rot}$, where ν_{rot} is the spinning frequency of the rotor.

polarization inversion during the SEMA period will greatly enhance the signals by a factor of about 2.[33,34] Even though PISEMA is widely used for the characterization of materials, there is still not any report about utilizing PISEMA related techniques to identify CH_n signals.

In this paper, we first propose using PISEMA NMR technique to efficiently distinguish CH_n carbon signals in organic solids on the basis of their completely different dipolar splitting line shapes as well as the characteristic splitting values. We first give a brief introduction to the theoretical background for our numerical simulations of the ^{13}C−^{1}H dipolar splitting patterns. Then, we have a detailed description on the procedures of identifying CH_n signals through the comparison of the individual characteristic line shapes and splitting values of the dipolar spitting patterns for different types of carbons. Finally, we demonstrate the feasibility of the method of identification on several typical solid small molecules, polymers, and biomacromolecules, which all excellently indicate the high efficacy of the method.

2. EXPERIMENTAL SECTION

Samples. L-alanine, glycine, and polymer samples were purchased from Aldrich Chemical Co., Inc. without further treatment. Cocoons of *B. mori* silkworm silk were commercially available.

Nuclear Magnetic Resonance (NMR) Experiments. Solid-state NMR experiments were performed on a Varian Infinityplus-400 spectrometer at a frequency of 100.5 MHz for ^{13}C and 399.7 MHz for ^{1}H. A conventional 4 mm double-resonance HX CP/MAS NMR probe was used, and samples were placed in a 4 mm zirconia PENCIL rotor with a 52 μL sample volume. The MAS was automatically controlled at 12 kHz within ±1 Hz with a MAS speed controller for all 1D and 2D NMR experiments. The ^{13}C chemical shifts were referenced to external HMB (hexamethylbenzene). The 2D PISEMA pulse sequence was used according to ref 28, where the Lee−Goldburg (LG) pulse sequence was adopted for proton homonuclear decoupling, and the radiofrequency power was relatively high at 79 kHz, corresponding to a 3.169 μs 90° pulse. Initial ^{13}C transverse magnetization was created by ramped ^{1}H−^{13}C CP, and the contact time was set as 0.6 ms. During the SEMA period, the ^{1}H effective field strength was 78.9 kHz with a resonance offset of 45.0 kHz. The ^{13}C field strengths were adjusted so that the difference in amplitude between the two RF fields was equal to $2\nu_{rot}$. Heteronuclear decoupling during the acquisition period was achieved by SPINAL-64 irradiation. The numerical simulations were performed using the SIMPSON programming package.[35] For most of the samples, overnight is long enough for acquiring a good PISEMA spectrum.

3. RESULTS AND DISCUSSION

As has been shown by Vega's group,[36,37] an approximate time-independent zero-order Hamiltonian operating in zero-quantum spin space is sufficient to describe the high-speed LG CP MAS evolution of carbon coherences, and then, the ^{13}C−^{1}H heteronuclear dipolar splitting patterns can be predicted by numerical simulations. In short, in a I_nS system of n protons I and one carbon S under the Hartmann−Hahn condition during the SEMA period, the effective Hamiltonian is given by[36]

$$H_1^* = \sum_i \frac{w_d^{(i)} \sin\theta_m}{4} G^{(i)} [I_i^+ S^- \exp(i\phi_i) + I_i^- S^+ \exp(-i\phi_i)]$$

where $G(i) = (3/4)\sin 2\theta_m \sin 2\theta_i$. Here, $w_d^{(i)}$ is the dipolar coupling constant, and (θ_i,ϕ_i) are polar angles in the rotor frame. Once the Hamiltonian is obtained, the signals for carbons can be calculated through powder averaging.

Actually, even though there are numerous CH_n chemical groups in a sample, their signals during the SEMA period can be explained quite satisfactorily using simple isolated models, such as the two-spin ^{13}CH, three-spin $^{13}CH_2$, and four-spin $^{13}CH_3$ models, as the covalent ^{13}C−^{1}H heteronuclear dipolar interactions play a dominant role during the dipolar coupling evolution period (t_1 period). It is reasonably postulated that the experimentally observed signals during the SEMA period are mainly due to powder averaging where the relaxation effect can be ignored, and thus, the signals can be simulated with small spin systems.[36] Indeed at a moderate MAS rate (10−14 kHz), CH_3, CH_2, and CH groups behave, to a large extent, as if they are effectively isolated from the surrounding proton reservoir.[17] Besides, PISEMA is a local-field technique, which is mainly used to detect the local microstructure and dynamics information. In addition, the resolution of the dipolar splitting spectrum is restricted by the ^{13}C line width, and the observed dipolar splittings are limited to one-bond ^{13}C−^{1}H and sometimes two-bond ^{13}C−^{13}C−^{1}H interactions.[38] Therefore, generally speaking, the powder-averaged signals of an isolated model could well be used to simulate the experimental results. In particular, it is the first time that we systematically study the difference of the individual characteristic line shapes of CH_n dipolar splitting patterns, which are further used to identify different types of carbon sites.

The result of numerical simulation is presented in Figure 2. It is noteworthy that there is a unique line shape of a dipolar splitting pattern and a corresponding characteristic splitting value for each carbon group, based on which different types of carbons can be distinguished unambiguously. For the CH_3 group, two pairs of obvious sharp peaks are clearly shown in the spectrum, with inner peaks higher than the outer ones in intensity. Generally, the dipolar splitting of the inner peaks is about 4 kHz due to fast rotations of the CH_3 group. As to the CH_2 group, a pair of sharp peaks with smooth shoulder peaks on the outside can be observed, and the shoulder peaks are not as sharp as those of CH_3. For the sharp peaks, the dipolar splitting value is larger than 10 kHz. For the CH group, the heteronuclear dipolar splitting pattern is only constituted of two symmetric sharp peaks, which looks similar to the Pake pattern,[39] except for the zero-frequency peak in the center, which can be ascribed to the ^{1}H off-resonance effect and remote weak dipolar interactions.[40] The dipolar splitting value is generally larger than 10 kHz due to its strong ^{13}C−^{1}H dipolar interactions. When it comes to

the quaternary carbons, due to the absence of covalent protons, the dipolar splitting comes from the weak dipolar interactions between the carbon and remote protons, and thus, the splitting value is much smaller at around 1−3 kHz, which makes it the easiest to identify. Therefore, below, we will mainly focus on the discussion of CH_3, CH_2, and CH groups in the point view of line shapes and dipolar splitting values of the $^{13}C-^{1}H$ heteronuclear dipolar patterns.

Although the simulation was done according to a common geometrical structure, a small change of bond length or angles will not result in an obvious change of the line shapes. It should be noted that our simulation results are based on the powder averaging of dipolar tensor orientations; therefore, it is only suitable for the solid powders without macroscopic molecular orientations. Local orientational order in the crystalline domain does not change the line shapes as there still are various heteronuclear dipolar tensor orientations on the whole. Thus, in general, the identification of CH_n signals can be achieved based on their unique dipolar splitting patterns and splitting values.

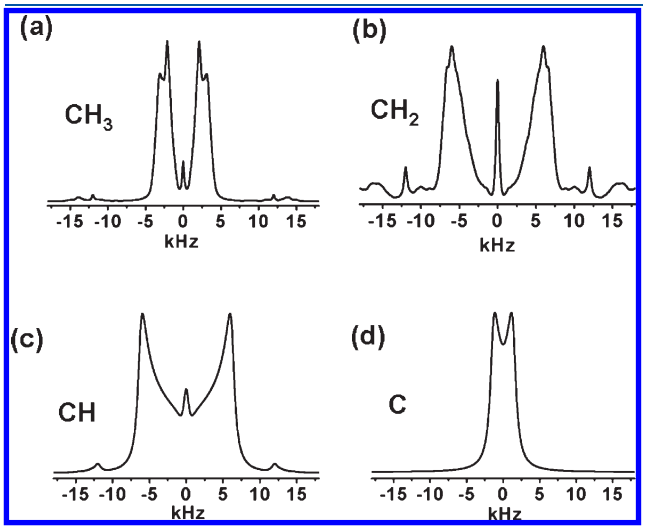

Figure 2. Numerical simulation of $^{13}C-^{1}H$ dipolar splitting patterns using the SIMPSON package[35] for (a) an isolated $^{13}CH_3$ group using a $^{13}C-^{1}H$ dipolar coupling constant of 7.5 kHz, where each $^{1}H-^{13}C-^{1}H$ angle is 109.5°; (b) an isolated $^{13}CH_2$ group using a $^{13}C-^{1}H$ dipolar coupling constant of 21.5 kHz, where the $^{1}H-^{13}C-^{1}H$ angle is 109.5°; (c) an isolated ^{13}CH group using a $^{13}C-^{1}H$ dipolar coupling constant of 22 kHz; and (d) a quaternary ^{13}C using a weak $^{13}C-^{1}H$ dipolar coupling constant of 5 kHz.

The high efficacy of this method of identifying CH_n signals is first demonstrated on the small organic molecules, such as L-alanine and glycine, as shown in Figure 3. As is expected, the line shapes of dipolar splitting patterns of the CH and CH_3 groups of L-alanine and the CH_2 group of glycine are all in good agreement with the prediction of our simulations. Due to the internal rotations, the inner splitting of the CH_3 dipolar splitting spectrum is about 4.2 kHz, much smaller than the dipolar splitting of CH (Figure 3a) and CH_2 groups (Figure 3b). In contrast, the dipolar splitting for CH and CH_2 groups is larger than 10 kHz due to the strong $^{13}C-^{1}H$ dipolar interactions. The peaks of quaternary carbons in L-alanine and glycine are easy to assign due to their much smaller dipolar splitting (data not shown). Also, they can be discriminated by their high chemical shift values, larger than 170 ppm, owing to the influence of the covalent connected oxygen atoms.

An excellent demonstration of the method applied in the polymer system is shown in Figure 4, where the same line shapes of CH_n dipolar splitting patterns are observed on a typical semicrystalline polymer, isotactic polypropylene (iPP). This iPP sample has a large number of crystalline domains with a crystallinity of about 44.4% (see Figure S1 in the Supporting Information). As expected, the line shapes of dipolar splitting patterns for the CH_n group are almost the same as our simulation results without suffering from the influence of local microscopic orientation order in the crystalline regions. Therefore, in general, our proposed method is also feasible on highly crystalline samples, as long as there are not any macroscopic molecular orientations in the sample. Also, it is clearly shown that the $^{13}C-^{1}H$ dipolar splitting value is about 4.5 kHz for the CH_3 group due to the internal rotations, while in CH and CH_2, the dipolar splitting value is more than 10 kHz from the spectra, much larger than that of the CH_3 group.

Also, we demonstrate that the method is feasible on biomacromolecules, such as silk fibroin, one of the most widely studied naturally abundant structural proteins.[41−43] The *Bombyx mori* silk fibroin contains a predominant repetitive sequence $(Gly-Ala-Gly-Ala-Gly-Ser)_n$ as well as small amounts of tyrosine and

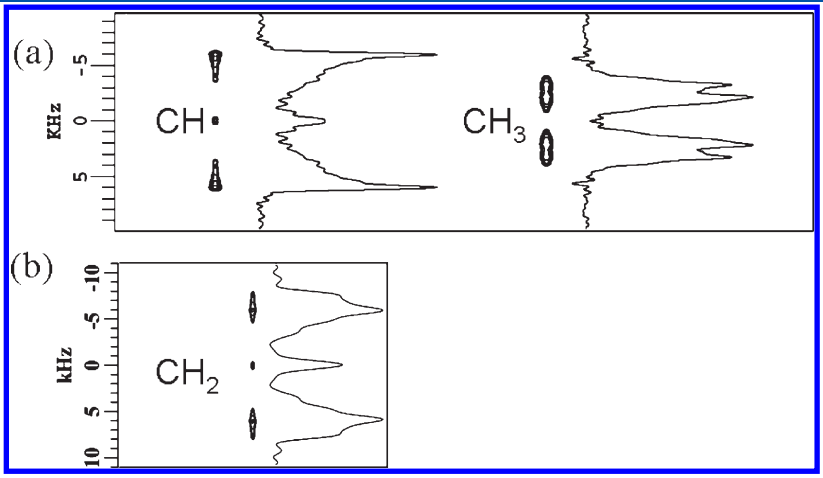

Figure 3. The $^{13}C-^{1}H$ 2D PISEMA spectra of (a) L-alanine and (b) glycine. The $^{13}C-^{1}H$ dipolar splitting patterns of CH_3, CH_2, and CH groups are also shown in the figure. Each experiment took only about 35 min.

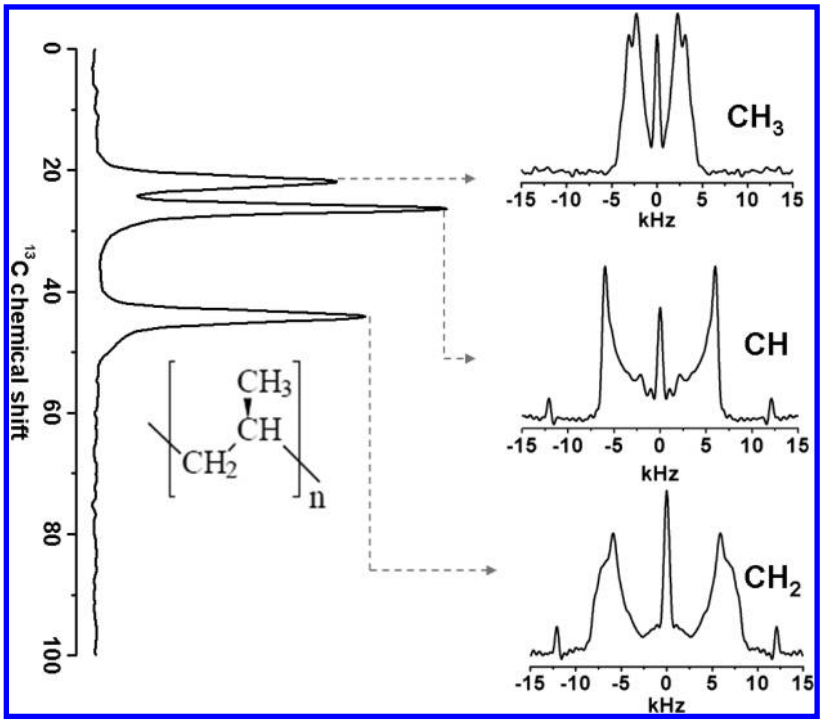

Figure 4. The ^{13}C CP/MAS spectrum of iPP as well as the $^{13}C-^{1}H$ dipolar splitting patterns sliced from the 2D PISEMA spectrum corresponding to CH_3, CH, and CH_2 groups from top to bottom. The PISEMA experiment took about 1.5 h.

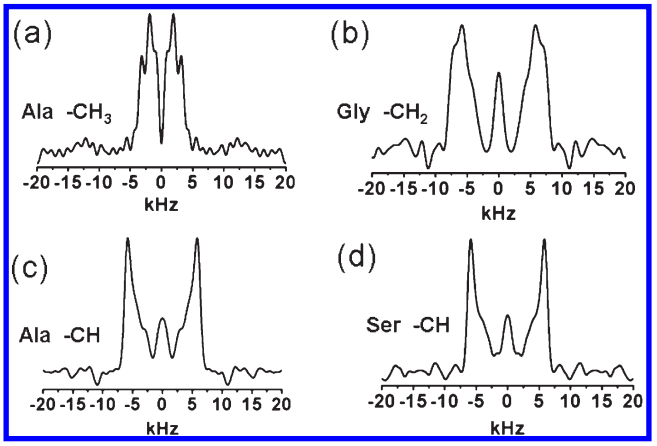

Figure 5. The $^{13}C-^{1}H$ dipolar splitting patterns sliced from the 2D PISEMA spectrum of naturally abundant silk fibroin, which corresponds to (a) CH_3 of alanine, (b) CH_2 of glycine, (c) CH of alanine, and (d) CH of serine. The PISEMA experiment took about 30 h.

valine.[44,45] The $^{13}C-^{1}H$ dipolar splitting spectra corresponding to different chemical groups are shown in Figure 5. As we expected, the line shapes of CH, CH_2, and CH_3 dipolar splitting patterns are all in a good agreement with our simulation results. The universality of our proposed method is further demonstrated on a series of solid polymers in Figures S2∼S16 in the Supporting Information.

The observation of the line shapes to identify CH_3, CH_2, and CH groups is usually based on the premise that each peak of the carbon groups can be well resolved. However, the overlap of peaks often occurs in solids, especially in polymer blends and copolymers.[46] A unique advantage of our proposed method is that the overlapped signals from different types of carbons can be easily distinguished based on the unique line shapes and dipolar splitting value of the $^{13}C-^{1}H$ dipolar splitting patterns. A typical example is the poly(methyl methacrylate)/poly(*p*-vinyl phenol) (PMMA/PVPh) blend, as shown in Figure 6, where all of the peaks are easily assigned except the peaks at about 45 and 53 ppm. As is shown, the inner dipolar splitting at 45 ppm (the red part in Figure 6c) is much smaller than the splitting of the CH_3 group of PMMA at about 17 ppm. Therefore, it should be ascribed to the signals of quaternary carbons in the backbone chain of PMMA. For the peak at 45 ppm, the outer dipolar splitting (the blue part in Figure 6c) is much larger than that of CH_3, more than 10 kHz. Judging from the line shape, it is reasonably ascribed to the signal of CH_2 in the backbone chain of PVPh. In addition, the line shape of the dipolar splitting pattern of the OCH_3 group in PMMA is slightly deformed due to the partial signal overlaps with the CH_2 group at about 53 ppm (see Figure S2, Supporting Information). However, the signal of the OCH_3 group can still be discriminated by the dipolar splitting values. Therefore, on the basis of the method of identifying different types of carbons by observing the dipolar splitting line shapes and values, we successfully make a clear assignment of each peak for the PMMA/PVPh blends, even though there are severe signal overlaps at 45 and 53 ppm.

One thing that deserves special attention is that the dipolar splitting patterns are obtained through the powder averaging of $^{13}C-^{1}H$ heteronuclear tensors with various directions to the magnetic field; therefore, to some extent, the above method may suffer from a limitation for samples with macroscopic molecular orientations, such as the liquid crystals or stretched polymers.[28] However, after a special sample treatment, such as a high-temperature quench, the macroscopic highly oriented samples may become quite disordered, and the CH_n signals may still be identified by the above method. Another special case that should be noted is the motions of aromatic rings, as shown in

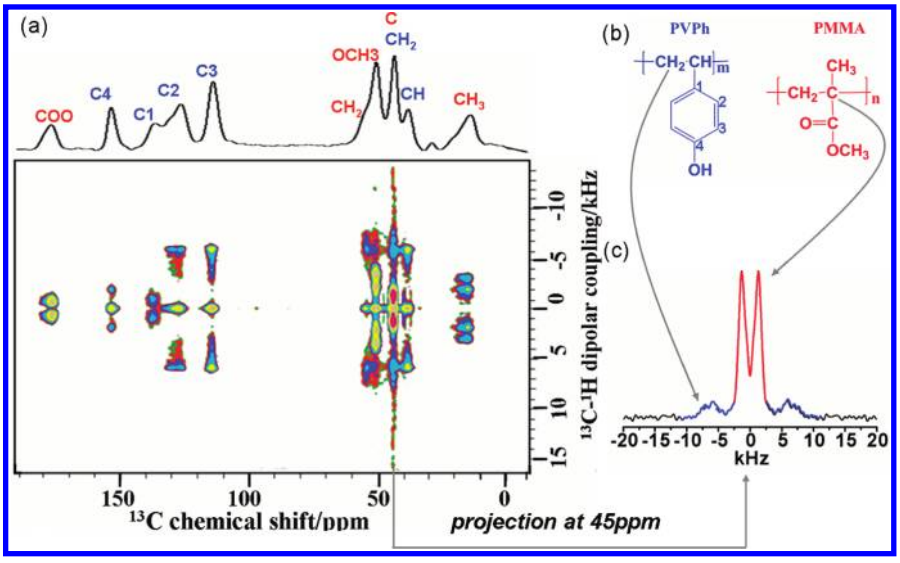

Figure 6. (a) The $^{13}C-^{1}H$ 2D PISEMA spectrum of the PMMA/PVPh blend with the ^{13}C dimensional projection on the top. The assignment of each peak was done according to our proposed method of identification. (b) The schematic diagram of the molecular structure of PMMA/PVPh blends. (c) The $^{13}C-^{1}H$ heteronuclear dipolar splitting pattern at about 45 ppm, indicative of the overlapped signals of quaternary carbons in the backbone chain of PMMA with CH_2 groups of PVPh. The PISEMA experiment took about 39 h.

Figures S15 and S16 (Supporting Information). Molecular motions, in particular, the flips and oscillations of aromatic rings, will have a large effect on the dipolar patterns, both in the value of the $^{13}C-^{1}H$ dipolar coupling and the line shapes of dipolar patterns.[33,47] However, it can still be easily identified by the general line shapes and slightly reduced splitting value, a bit less than 8 kHz. It should be emphasized that sometimes, only a quick look at the 2D PISEMA contour plot instead of the slices is enough to identify different carbons according to their characteristic 2D contour pattern as shown in Figure 3 and 6. In addition, the dipolar splitting patterns may be a little different for the same chemical groups in different samples, which could, to an extent, be ascribed to the surrounding different chemical environment as well as the various dynamic behaviors. In particular, the dynamic behaviors of the components in polymer blends could be quite different from the neat polymer component.[48−50] Generally, the change of dynamic behaviors will result in different heteronuclear dipolar coupling; therefore, more information about dynamical behaviors upon mixing could be observed from the comparison of the dipolar patterns and dipolar splitting values.

4. CONCLUSION

In conclusion, on the basis of the combination of numerical simulations and experimental demonstrations, we first proposed using the PISEMA NMR technique to identify different types of carbon signals in organic solids by utilizing the characteristic line shapes and the dipolar splitting values of the $^{13}C-^{1}H$ dipolar splitting patterns. Moreover, this method is well-suited to identify completely overlapped signals for different types of carbons. Furthermore, overnight is long enough to get a high-quality PISEMA spectrum for most of the samples. The efficacy of this method was well demonstrated on typical solid small molecules, polymers, and biomacromolecules. We believe that the PISEMA NMR technique is a fairly reliable approach to identify different types of carbons in organic solids, which may enjoy great popularity for chemists in various scientific fields in the future.

■ ASSOCIATED CONTENT

Supporting Information. The DSC curve of iPP and $^{13}C-^{1}H$ dipolar splitting patterns of CH_3, CH_2, and CH groups for a series of solid polymers. This material is available free of charge via the Internet at http://pubs.acs.org.

■ AUTHOR INFORMATION

Corresponding Author

*E-mail: spclbh@nankai.edu.cn (P.S.); baohui@nankai.edu.cn (B.L.).

■ ACKNOWLEDGMENT

This work was supported by the National Science Fund for Distinguished Young Scholars (No. 20825416) and the National Natural Science Foundation of China (NSFC) through the General Programs (No. 20774054).

■ REFERENCES

(1) Bovey, F. A.; Mirau, P. A. *NMR of Polymers*; Academic Press: New York, 1996.
(2) Gan, Z. H.; Madhu, P. K.; Amoureux, J. P.; Trebosc, J.; Lafon, O. *Chem. Phys. Lett.* **2011**, *503*, 167.
(3) Schmidt-Rohr, K.; Spiess, H. W. *Multidimensional Solid-State NMR and Polymers*; Academic Press: London, 1994.
(4) Brus, J.; Urbanova, M. *J. Chem. Phys. A* **2005**, *109*, 5050.
(5) Sun, P. C.; Dang, Q. Q.; Li, B. H.; Chen, T. H.; Wang, Y. N.; Lin, H.; Jin, Q. H.; Ding, D. T.; Shi, A. C. *Macromolecules* **2005**, *38*, 5654.
(6) Wolak, J. E.; Knutson, J.; Martin, J. D.; Boyle, P.; Sargent, A. L.; White, J. L. *J. Phys. Chem. B* **2003**, *107*, 13293.
(7) Zhu, H.; Graf, R.; Hou, G.; Zhao, Y.; Wang, D.; Spiess, H. W. *Macromol. Chem. Phys.* **2010**, *211*, 1157.
(8) Saalwachter, K. *Prog. Nucl. Magn. Reson. Spectrosc.* **2007**, *51*, 1.
(9) Patt, S. L.; Shoolery, J. N. *J. Magn. Reson.* **1982**, *46*, 535.
(10) Ernst, R. R.; Bodenhausen, G.; Wokaun, A. *Principles of Nuclear Magnetic Resonance in One and Two Dimensions*; Clarendon Press: Oxford, 1987.
(11) Lesage, A.; Steuernagel, S.; Emsley, L. *J. Am. Chem. Soc.* **1998**, *120*, 7095.

(12) Sakellariou, D.; Lesage, A.; Emsley, L. *J. Magn. Reson.* **2001**, *151*, 40.
(13) Burns, S. T.; Wu, X.; Zilm, K. W. *J. Magn. Reson.* **2000**, *143*, 352.
(14) Wu, X. L.; Burns, S. T.; Zilm, K. W. *J. Magn. Reson. A* **1994**, *111*, 29.
(15) Wu, X. L.; Zilm, K. W. *J. Magn. Reson. A* **1993**, *104*, 119.
(16) Wu, X. L.; Zilm, K. W. *J. Magn. Reson. A* **1993**, *102*, 205.
(17) De Vita, E.; Frydman, L. *J. Magn. Reson.* **2001**, *148*, 327.
(18) Saalwachter, K.; Graf, R.; Spiess, H. W. *J. Magn. Reson.* **2001**, *148*, 398.
(19) Schmidt-Rohr, K.; Mao, J. D. *J. Am. Chem. Soc.* **2002**, *124*, 13938.
(20) Mao, J. D.; Schmidt-Rohr, K. *J. Magn. Reson.* **2005**, *176*, 1.
(21) Hester, R. K.; Ackerman, J. L.; Neff, B. L.; Waugh, J. S. *Phys. Rev. Lett.* **1976**, *36*, 1081.
(22) Munowitz, M. G.; Griffin, R. G.; Bodenhausen, G.; Huang, T. H. *J. Am. Chem. Soc.* **1981**, *103*, 2529.
(23) Munowitz, M. G.; Griffin, R. G. *J. Chem. Phys.* **1982**, *76*, 2848.
(24) Wu, C. H.; Ramamoorthy, A.; Opella, S. J. *J. Magn. Reson. A* **1994**, *109*, 270.
(25) Ramamoorthy, A.; Opella, S. J. *Solid State Nucl. Magn. Reson.* **1995**, *4*, 387.
(26) Nevzorov, A. A.; Opella, S. J. *J. Magn. Reson.* **2003**, *164*, 182.
(27) Wu, C. H.; Opella, S. J. *J. Magn. Reson.* **2008**, *190*, 165.
(28) Dvinskikh, S. V.; Zimmermann, H.; Maliniak, A.; Sandstrom, D. *J. Magn. Reson.* **2003**, *164*, 165.
(29) Dvinskikh, S. V.; Zimmermann, H.; Maliniak, A.; Sandström, D. *J. Magn. Reson.* **2003**, *163*, 46.
(30) Marassi, F. M.; Opella, S. J. *J. Magn. Reson.* **2000**, *144*, 150.
(31) Denny, J. K.; Wang, J.; Cross, T. A.; Quine, J. R. *J. Magn. Reson.* **2001**, *152*, 217.
(32) Ramamoorthy, A.; Wei, Y. F.; Lee, D. K. *Annu. Rep. NMR. Spectrosc.* **2004**, *52*, 4103.
(33) Hong, M.; Yao, X.; Jakes, K.; Huster, D. *J. Phys. Chem. B* **2002**, *106*, 7355.
(34) Sinha, N.; Ramanathan, K. V. *Chem. Phys. Lett.* **2000**, *332*, 125.
(35) Bak, M.; Rasmussen, J. T.; Nielsen, N. C. *J. Magn. Reson.* **2000**, *147*, 296.
(36) Ladizhansky, V.; Vega, S. *J. Chem. Phys.* **2000**, *112*, 7158.
(37) van Rossum, B.-J.; CP, d. G.; Ladizhansky, V.; Vega, S. *J. Am. Chem. Soc.* **2000**, *122*, 3465.
(38) Fung, B. M. *Prog. Nucl. Magn. Reson. Spectrosc.* **2002**, *41*, 171.
(39) Pake, G. E. *J. Chem. Phys.* **1948**, *16*, 327.
(40) Dvinskikh, S. V.; Sandström, D. *J. Magn. Reson.* **2005**, *175*, 163.
(41) Wang, M.; Jin, H.-J.; Kaplan, D. L.; Rutledge, G. C. *Macromolecules* **2004**, *37*, 6856.
(42) Shao, Z.; Vollrath, F. *Nature* **2002**, *418*, 741.
(43) Hu, B. W.; Zhou, P.; Noda, I.; Ruan, Q. X. *J. Phys. Chem. B* **2006**, *110*, 18046.
(44) Dang, Q.; Lu, S.; Yu, S.; Sun, P.; Yuan, Z. *Biomacromolecules* **2010**, *11*, 1796.
(45) White, J. L.; Wang, X. W. *Macromolecules* **2002**, *35*, 2633.
(46) Zhang, X.; Takegoshi, K.; Hikichi, K. *Macromolecules* **1991**, *24*, 5756.
(47) Schaefer, J.; Stejskal, E. O.; McKay, R. A.; Dixon, W. T. *Macromolecules* **1984**, *17*, 1479.
(48) Wachowicz, M.; Gill, L.; Wolak, J.; White, J. L. *Macromolecules* **2008**, *41*, 2832.
(49) Gill, L.; Damron, J.; Wachowicz, M.; White, J. L. *Macromolecules* **2010**, *43*, 3903.
(50) Wolak, J. E.; White, J. L. *Macromolecules* **2005**, *38*, 10466.